Magneto-nanofluid flow with heat transfer past a stretching surface for the new heat flux model using numerical approach

Noreen Sher Akbar
DBS&H CEME, National University of Sciences and Technology, Islamabad, Pakistan

O. Anwar Beg
Biofluid Mechanics, Spray Research Group, School of Computing, Science and Engineering, University of Salford–Manchester, Manchester, UK, and

Z.H. Khan
Department of Mathematics, University of Malakand, Chakdara, Pakistan

Received 23 March 2016
Revised 20 April 2016
Accepted 25 April 2016

Abstract

Purpose – Sheet processing of magnetic nanomaterials is emerging as a new branch of smart materials' manufacturing. The efficient production of such materials combines many physical phenomena including magnetohydrodynamics (MHD), nanoscale, thermal and mass diffusion effects. To improve the understanding of complex inter-disciplinary transport phenomena in such systems, mathematical models provide a robust approach. Motivated by this, this study aims to develop a mathematical model for steady, laminar, MHD, incompressible nanofluid flow, heat and mass transfer from a stretching sheet.

Design/methodology/approach – This study developed a mathematical model for steady, laminar, MHD, incompressible nanofluid flow, heat and mass transfer from a stretching sheet. A uniform constant-strength magnetic field is applied transversely to the stretching flow plane. The *Buongiorno* nanofluid model is used to represent thermophoretic and Brownian motion effects. A non-Fourier (Cattaneo–Christov) model is used to simulate thermal conduction effects, of which the Fourier model is a special case when thermal relaxation effects are neglected.

Findings – The governing conservation equations are rendered dimensionless with suitable scaling transformations. The emerging nonlinear boundary value problem is solved with a fourth-order Runge–Kutta algorithm and also shooting quadrature. Validation is achieved with earlier non-magnetic and forced convection flow studies. The influence of key thermophysical parameters, e.g. Hartmann magnetic number, thermal Grashof number, thermal relaxation time parameter, Schmidt number, thermophoresis parameter, Prandtl number and Brownian motion number on velocity, skin friction, temperature, Nusselt number, Sherwood number and nanoparticle concentration distributions, is investigated.

Originality/value – A strong elevation in temperature accompanies an increase in Brownian motion parameter, whereas increasing magnetic parameter is found to reduce heat transfer rate at the wall (Nusselt number). Nanoparticle volume fraction is observed to be strongly suppressed with greater thermal Grashof number, Schmidt number and thermophoresis parameter, whereas it is elevated significantly with greater Brownian motion parameter. Higher temperatures are achieved with greater thermal relaxation time values, i.e. the non-Fourier model predicts greater values for temperature than the classical Fourier model.

Keywords Brownian motion, Boundary layer flow, Magnetic nanofluids, Non-Fourier conduction

Paper type Research paper

International Journal of Numerical Methods for Heat & Fluid Flow
Vol. 27 No. 6, 2017
pp. 1215-1230

0961-5539
DOI 10.1108/HFF-03-2016-0125

Nomenclature

C = Nanoparticle (solutal) concentration
C_w = Nanoparticle (solute) concentration at the wall
C_∞ = Ambient nanoparticle concentration as y tends to infinity
D_B = Brownian diffusion coefficient
D_T = Thermophoretic diffusion coefficient
B_0 = Magnitude of magnetic field strength
T = Local fluid temperature
T_∞ = Ambient temperature
u, v = Velocity components along x and y directions
P = Pressure
ϕ = Nanoparticle volume fraction
η = Similarity variable (transformed coordinate)
Nu_x = Local Nusselt number
Sh_x^n = Local nanoparticle Sherwood number
$(\rho c)_p$ = Effective heat capacity of the nanoparticle material
θ = Dimensionless temperature
γ = Non-dimensional thermal relaxation time
q = Heat flux
G_T = Thermal Grashof number
g = Acceleration due to gravity
λ_2 = Thermal relaxation time
B_C = Solutal Grashof number
ν = Kinematic viscosity of the fluid
P_r = Prandtl number
M = Hartmann Number
N_b = Brownian motion parameter
Sc = Schmidt number (= P_rLe)
Re_x = Local Reynolds number
μ = Dynamic viscosity of nanofluid
Le = Regular Lewis number
x, y = Coordinate along and normal to the sheet
$(\rho c)_f$ = Heat capacity of the fluid
N_t = Thermophoresis parameters
K = Thermal conductivity of the fluid

1. Introduction

Nanoparticles provide a bridge between bulk materials and molecular structure. When deployed strategically in base fluids, the resulting "nanofluids" have been proven to achieve exceptional enhancement in thermal conductivity properties, as identified by Choi (1995). This has made them attractive in numerous areas of modern technology including aerospace cooling systems (Narvaez *et al.*, 2014), heat exchangers (Huminic and Huminic, 2012) and energy systems (Bég *et al.*, 2011). When developing customized nanofluids for deployment in such applications, manufacturing processes exert a key influence on the constitution of final products. In materials processing a popular mechanism used is that of *continuous sheet stretching*. The mathematical study of such flows was mobilized over five decades ago by Sakiadis (1961) who considered Newtonian flows from continuously moving surfaces. This type of flow is particularly suitable for simulation with the *boundary layer theory*. Many subsequent studies have appeared examining heat and mass transfer in stretching boundary

layer flows including Takhar *et al.* (1998), Gorla and Sidawi (1994) and Togun *et al.* (2015). More recently, nanofluid stretching boundary layer flows have also been considered and representative works include studies of Uddin *et al.* (2015), Rana and Bhargava (2012), Nadeem *et al.* (2013) and Rana *et al.* (2013). The two most popular approaches in simulating nanofluid boundary layer transport phenomena are either the *Buongiorno model* (which invokes a separate species concentration boundary layer equation) and the *Tiwari–Das* model (which only requires momentum and energy boundary layer equations and simulates nanoparticle effects via a volume fraction parameter). Many researchers have used these approaches including Nield and Kuznetsov (2009), Rashidi *et al.* (2014), Latiff *et al.* (2016) and Ferdows *et al.* (2014). The vast majority of such studies have considered the classical Fourier model for thermal conduction heat transfer. However, it has been identified that this model may not be accurate for certain situations, as it produces a *parabolic energy equation*, which implies that any initial thermal disturbance is instantly experienced by the medium under examination. A modification to the Fourier law is therefore necessitated, and in this regard, a robust model that has been proposed is the *Cattaneo–Christov non-Fourier model* (Cattaneo, 1948; Christov, 2009; Straughan, 2010). This features a relaxation time for heat flux and results in a *hyperbolic energy equation* that successfully captures the flux of heat via propagation of thermal waves with finite speed. It is relevant to not only materials processing operations (Han *et al.*, 2014) but also bio-heat transfer (Elsayed and Anwar Bég, 2014). A number of excellent studies have appeared recently using the *Cattaneo–Christov non-Fourier model* including Mustafa (2015) who studied rotating viscoelastic heat transfer and Sheikholeslami *et al.* (2014d) who investigated melting in stretching sheet flow of a non-Newtonian fluid.

Magnetohydrodynamics (MHD) is the study of the interaction of magnetic fields (which may be either static or oscillating) and electrically conducting fluids. It is a subject of immense industrial importance in, for example, metallurgical processing and induction furnaces (Frizen and Sarapulov, 2010). MHD also has significant emerging applications in biomagnetic flow control (Bhargava *et al.*, 2010), Marangoni convection in biophysical suspensions (Bég *et al.*, 2014a), hemodynamics (Hoque *et al.*, 2013) and pharmacodynamics (Bég *et al.*, 2014c). In pharmacodynamics, it has also been exploited in targeted drug delivery, where nanoparticles are coated in magnetic materials to assist in their direct ability in the human circulatory system. Furthermore, in nuclear engineering systems (Kim *et al.*, 2007), magnetic nanofluids are also being examined, as they combine both the thermal enhancement properties of nanofluids and the magnetic manipulation properties of electrically conducting liquids. The former can assist in, for example, cooling very-high-temperature surfaces and the latter permits manipulation of flow rates and also heat transfer characteristics (Buongiorno and Hu, 2007). It is therefore beneficial to investigate the thermofluid dynamics of magnetic nanofluid sheet processing, as this provides further insight into the heat transfer, mass transfer and momentum characteristics of nanomaterials. The investigation of non-Fourier heat conduction phenomena also gives a more realistic appraisal of thermomechanics of nanofluids (Ciarletta and Straughan, 2010) which may be exploited strategically in reducing heat transfer rates of nuclear power technologies (both for civilian and future aerospace propulsion). Such analyses may also be of use in minimizing overheating of hybrid deep-space rocket propulsion systems (Bég *et al.*, 2014b). Further recent literature can be viewed through Buongiorno (2006), Prasad *et al.* (2015), Salahuddin *et al.* (2016), Akbar *et al.* (2015, 2016, 2012), Khan *et al.* (2014), Khan and Pop (2010), Wang (1989), Kandasamy *et al.* (2011), Nadeem *et al.* (2015), Sheikholeslami *et al.* (2014a, 2014b, 2014c, 2014e), Zeeshan *et al.* (2016), Ellahi *et al.* (2014).

In the present study, we therefore theoretically examine, for the first time, the steady, laminar, MHD, incompressible nanofluid flow, heat and mass diffusion from a stretching sheet,

as a model of magnetic nanomaterials fabrication. We adopt the Buongiorno (2006) nanofluid model, which emphasizes thermophoretic and Brownian motion effects and introduces a separate nanoparticle species diffusion equation. The Cattaneo–Christov non-Fourier thermal conduction model has also been applied (Sheikholeslami *et al.*, 2014c), which introduces a thermal relaxation effect. The normalized non-linear, two-point boundary value problem is solved with numerical shooting quadrature. Validation with previous studies is included. The current study has, to the best of our knowledge, not appeared in the literature thus far.

2. Mathematical flow model

The regime under investigation is illustrated in Figure 1. Two-dimensional, steady-state, incompressible flow of an electrically conducting nanofluid from a vertical stretching sheet is considered, with reference to an (x, y) coordinate system, where the x-axis is aligned with the sheet. A transverse static uniform-strength magnetic field is applied, which is sufficiently weak to negate magnetic induction and Hall current effects. The nanofluid is dilute and comprises a homogenous suspension of equally sized nanoparticles in thermal equilibrium. The sheet is stretched in the plane $y = 0$. The flow is assumed to be confined to $y > 0$. Here, we assumed that the sheet is uniformly extended with the linear velocity $u(x) = ax$, where $a > 0$ is constant and x-axis is measured along the stretching surface. Under these assumptions, the governing conservation equations for mass, momentum, energy (heat) and nanoparticle species diffusion, neglecting viscous and Joule dissipation effects, may be shown to take the following form:

$$\frac{\partial u}{\partial x} + \frac{\partial v}{\partial y} = 0 \tag{1}$$

$$\left(u\frac{\partial u}{\partial x} + v\frac{\partial u}{\partial y}\right) = \nu\left(\frac{\partial^2 u}{\partial y^2}\right) - \frac{\sigma B_o^2}{\rho}u + \rho g\beta_T(T - T_\infty) + \rho g\beta_C(C - C_\infty) \tag{2}$$

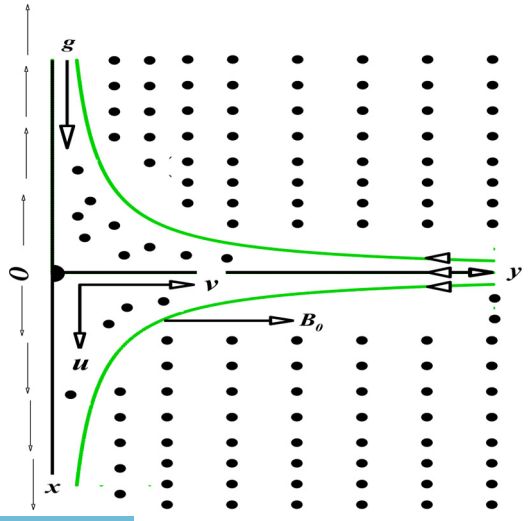

Figure 1.
Physical model for the MHD nanofluid stretching sheet problem

$$\rho(c_p)\bar{v}\cdot\nabla T = -\nabla\cdot q + \tau\left[D_B\frac{\partial T}{\partial y}\frac{\partial C}{\partial y} + \left(\frac{D_T}{T_\infty}\right)\left(\frac{\partial T}{\partial y}\right)^2\right] \tag{3}$$

$$\left(u\frac{\partial \phi}{\partial x} + v\frac{\partial \phi}{\partial y}\right) = D_B\frac{\partial^2 C}{\partial y^2} + \left(\frac{D_T}{T_\infty}\right)\frac{\partial^2 T}{\partial y^2} \tag{4}$$

Here $\tau = \frac{(\rho c)_p}{(\rho c)_f}$ is the ratio of the effective heat capacity of the nanoparticles to the base fluid; u and v are the velocity components along the x and y directions, respectively; T is the temperature of the magnetic nanofluid; B_0 is the magnitude of magnetic field strength; and q is the heat flux. In equation (3), we use the Cattaneo–Christov thermal conduction model for heat flux, which has the following form:

$$q + \lambda_2\left(\frac{\partial q}{\partial t} + V\cdot\nabla\cdot q - q\cdot\nabla V + (\nabla\cdot V)q\right) = -K\nabla T \tag{5}$$

Here λ_2 is the *thermal relaxation time*. Eliminating q from equations (3) and (5), the modified energy conservation equation then assumes the form:

$$\left(u\frac{\partial T}{\partial x} + v\frac{\partial T}{\partial y}\right) + \lambda_2\left(u\frac{\partial u}{\partial x}\frac{\partial T}{\partial x} + v\frac{\partial v}{\partial y}\frac{\partial T}{\partial y} + u\frac{\partial v}{\partial x}\frac{\partial T}{\partial y} + v\frac{\partial u}{\partial y}\frac{\partial T}{\partial x} + 2uv\frac{\partial^2 T}{\partial x\partial y} + u^2\frac{\partial^2 T}{\partial x^2} + v^2\frac{\partial^2 T}{\partial y^2}\right) = \frac{K}{\rho(c_p)}\frac{\partial^2 T}{\partial y^2} + \tau\left[D_B\frac{\partial T}{\partial y}\frac{\partial C}{\partial y} + \left(\frac{D_T}{T_\infty}\right)\left(\frac{\partial T}{\partial y}\right)^2\right] \tag{6}$$

Here T is the nanofluid temperature and P is the pressure, and the other physical quantities are defined in the nomenclature. We note that when $\lambda_2 \to 0$, the thermal relaxation effect is negated and the Cattaneo–Christov thermal conduction model is reduced to the *classical Fourier conduction law*. Essentially, therefore, the presence of thermal relaxation makes the energy conservation equation a *non-Fourier* model. The boundary conditions are prescribed as follows:

$$u = u_w(x) = ax,\ v = 0,\ T = T_w,\ C = C_w,\ \text{at y } = 0 \tag{8}$$

$$u \to 0,\ v \to 0,\ T \to T_\infty,\ C \to C_\infty,\ \text{as } y \to \infty \tag{9}$$

To facilitate numerical solutions to the primitive boundary value problem, it is pertinent to introduce the following similarity transformations and dimensionless variables:

$$u = axf'(\eta),\ v = -\sqrt{(a\nu)}f(\eta),\ \ \eta = \sqrt{\left(\frac{a}{\nu}\right)}y,\ \ \theta(\eta) = \frac{T - T_\infty}{T_w - T_\infty},\ \ \phi(\eta) = \frac{C - C_\infty}{C_w - C_\infty} \tag{10}$$

Implementing equation (9) in the conservation equations (1), (2), (4) and (6), the following nonlinear, coupled system of self-similar ordinary differential equations emerges:

$$f''' - (f')^2 + ff'' - M^2 f' + G_r\theta + B_r\Phi = 0 \tag{11}$$

$$\frac{1}{\Pr}\theta'' + f\theta' + N_b\theta'\xi' + N_t(\theta')^2 - \gamma\left(ff'\theta' + f^2\theta''\right) = 0 \tag{12}$$

$$\phi'' + Scf\,\phi' + \frac{N_t}{N_b}\theta'' = 0 \tag{13}$$

The transformed boundary conditions assume the form:

$$f(0) = 0, f'(0) = 1,\ \theta(0) = 1,\ \phi(0) = 1 \tag{13a}$$

$$f'(\infty) = 0,\ \ \theta(\infty) = 0,\ \ \phi(\infty) = 0 \tag{13b}$$

Where primes denote differentiation with respect to η, i.e. the transformed transverse coordinate. Furthermore the following dimensionless numbers are invoked in equations (10)-(12):

$$M^2 = \frac{\sigma {B_0}^2}{\rho a},\ R_{ex} = \frac{u_w(x)x}{\nu},\ G_T = \frac{\rho g x^3 \beta_T (T_w - T_\infty)}{\nu^2},\ G_r = \frac{G_T}{{R_{ex}}^2}$$

$$\Pr = \frac{\nu}{\alpha},\ N_b = \frac{\tau D_B(\phi_w - \phi_\infty)}{\nu},\ N_t = \frac{\tau D_T(T_w - T_\infty)}{\nu T_\infty},\ Sc = PrLe,\ \gamma = a\lambda_2 \tag{14}$$

$$B_T = \frac{\rho g x^3 \beta_C (C_w - C_\infty)}{\nu^2},\ B_r = \frac{B_T}{{R_{ex}}^2}$$

These represent the square of *Hartmann magnetic body force number, local Reynolds number, thermal Grashof number* (ratio of *thermal buoyancy force* to *viscous force*, *thermal buoyancy ratio parameter, Prandtl number, Brownian motion parameter, thermophoresis parameter, Schmidt number, thermal relaxation parameter, solutal [species] Grashof number* [ratio of *concentration buoyancy force* to *viscous force*]) and *species buoyancy ratio parameter*. Expressions for the skin friction coefficient (wall shear stress function), local Nusselt number (wall heat transfer rate) and the local Sherwood number (wall nanoparticle mass transfer rate) may also be defined as follows:

$$C_f = \frac{\tau_w}{\rho {u_w}^2}, Nu = \frac{x q_w}{\alpha(T_w - T_\infty)},\ Sh = \frac{x q_m}{\alpha(C_w - C_\infty)} \tag{15}$$

$$\tau_w = \mu\left(\frac{\partial u}{\partial y}\right),\ q_w = -\alpha\left(\frac{\partial T}{\partial y}\right),\ q_m = -\alpha\left(\frac{\partial C}{\partial y}\right) \tag{16}$$

$${\mathrm{Re}_x}^{1/2} C_f = f''(0),\ {\mathrm{Re}_x}^{-1/2} Nu_x = -\theta'(0),\ {\mathrm{Re}_x}^{-\frac{1}{2}} Sh_x = -\phi'(0) \tag{17}$$

It is important to note that the present boundary value problem reduces to the classical problem of MHD flow and the heat and mass transfer owing to a stretching surface in a viscous fluid when N_b and $N_t \rightarrow 0$ neglecting nanoscale effects, in equation (10) and equation (11). Furthermore, the non-Fourier model contracts to the classical Fourier model when $\gamma \rightarrow 0$, i.e. thermal relaxation time effects vanish. The functions defined in equations (15)-(17) provide an important estimate of the wall heat and mass transfer characteristics which are useful in materials' processing design.

3. Numerical solutions of transformed equations and validation

The nonlinear ordinary differential equations (10)-(12) subject to the boundary condition equation (13) have been solve numerically using an efficient Runge–Kutta fourth-order method along with a shooting technique. The asymptotic boundary conditions given by equation (13) were replaced by using a value of 15 for the similarity variable $\eta_{\max}$. The choice of $\eta_{\max} = 15$ and the step size $\Delta\eta = 0.001$ ensured that all numerical solutions approached the asymptotic values correctly. For validation of the proposed scheme, a comparison for the Nusselt number with the literature has been shown in Table I, for the MHD case without thermal buoyancy. Furthermore, additional benchmarking of solutions has been documented in Table II. Very good correlation is achieved for all values of Hartmann number (M) in Table I and for all Prandtl numbers (P_r) in Table II with published solutions.

In these tables, skin friction is shown to decrease significantly with greater M value, whereas Nusselt number is observed to be consistently elevated with greater P_r value (which is a thermophysical property of a particular fluid). The former is attributable to the decelerating effect of magnetic field via the Lorentzian MHD drag. The latter is caused by the decrease in thermal conductivity of fluids with greater Prandtl number which enhances heat transfer to the wall, reduces temperatures in the body of the fluid and thereby elevates Nusselt number. Therefore, we are confident that the applied numerical scheme is very accurate.

M	Present results	Salahuddin *et al.* (2016)	Akbar *et al.* (2015)
0.0	1	1	1
0.5	−1.11803	−1.11801	−1.11803
1	−1.41421	−1.41418	−1.41421
5	−2.44949	−2.44942	−2.44949
10	−3.31663	−3.31656	−3.31663
100	−10.04988	−10.04981	−10.04988
500	−22.38303	−22.38393	−22.38303
1,000	−31.63859	−31.63846	−31.63859

Table I. Comparison of results for skin friction for ($G_r = 0$)

P_r	Present results	Khan *et al.* (2014)	Khan and Pop (2010)	Wang (1989)	Kandasamy *et al.* (2011)
0.07	0.0663	0.0663	0.0663	0.0656	0.0661
0.20	0.1691	0.1691	0.1691	0.1691	0.1691
0.70	0.4539	0.4539	0.4539	0.4539	0.4542
2	0.9114	0.9114	0.9113	0.9114	0.9114
7	1.8954	1.8954	1.8954	1.8954	1.8952
20	3.3539	3.3539	3.3539	3.3539	–
70	6.4622	6.4622	6.4621	6.4622	–

Table II. Comparison of results for Nusselt number for pure fluid, i.e., $N_t = N_b = 0$, with $M = 0$, $\gamma = 0$ and $G_r = 0$

4. Results and discussion

Extensive numerical computations have been conducted. The results are depicted in Figures (2)-(7), in which the influence of selected parameters on momentum, heat and mass transfer characteristics is presented graphically.

Evidently, a significant acceleration accompanies an increase in thermal buoyancy ratio (G_r), as the thermal buoyancy (free convection current) effect aids momentum diffusion in the boundary layer. G_r, in fact, defines the ratio of thermal Grashof number to the square of Reynolds number and invokes therefore not just thermal buoyancy force and viscous force but also inertial force. Thermal buoyancy encourages flow but reduces the momentum boundary layer thickness. It is therefore a primary mechanism used in materials processing operations to generate greater momentum flux. Conversely, increasing Hartmann number, which symbolizes the relative contribution of *Lorentzian* MHD *drag force* to *viscous hydrodynamic force*, results in a strong deceleration in nanofluid boundary layer flow. The velocity is therefore markedly decreased with greater M value and the momentum boundary layer thickness is increased.

The asymptotically smooth profiles computed in Figure 2 also testify to the selection of an adequately large infinity boundary condition. Velocity profiles descend sharply from the sheet surface, indicating that there is a deceleration in the nanofluid flow for relatively short migration into the thickness of the boundary layer. The weak nature of the magnetic field ($M = 2$ is the maximum Hartmann number studied and corresponds to the Lorentzian force being double the viscous force) manifests in a distinct absence of any velocity overshoot at or near the wall.

Figure 3(a)-(c) illustrates the collective effects of several key parameters on temperature distribution, $\theta(\eta)$. Evidently, in Figure 3(a), a marked enhancement in temperature accompanies a rise in Hartmann number. The supplementary work expended in dragging the nanofluid against the imposed transverse magnetic field is dissipated as thermal energy. This results in a heating of the nanofluid regime and an increase in thermal boundary layer thickness. With increasing thermal buoyancy ratio, however, there is a slight depletion in temperatures. Thermal buoyancy force is known to cool the boundary layer flows while simultaneously accelerating them. In Figure 3(b), we observe that an increase in Brownian motion parameter (N_b) strongly elevates temperatures. Larger magnitudes of N_b physically corresponds to smaller particles and vice versa for smaller values of N_b. Smaller particles are

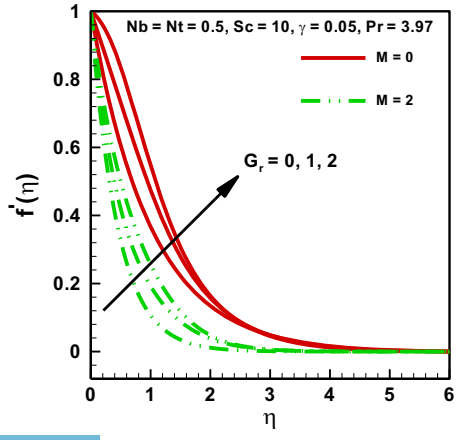

Figure 2.
Velocity profile for different values of thermal buoyancy ratio (G_r) and Hartmann number (M)

able to enhance thermal conduction in the nanoscale, and this globally results in an increase in the bulk temperature of the fluid, as highlighted by Choi (1995) and later by Buongiorno (2006). Although other mechanisms may contribute to thermal conductivity enhancement such as ballistic collisions and macro-convection, one of the dominant mechanisms (certainly for laminar flows) is now believed to be Brownian motion. The influence of the other key mechanisms, namely, thermophoresis, is also depicted in Figure 3(b). Greater values of thermophoresis parameter (N_t) are also observed to elevate temperatures and therefore increase thermal boundary layer thickness. Thermophoresis encourages nanoparticle transport away from a hotter surface towards a colder zone. This results in the transport of thermal energy to the body of nanofluid, thus increasing temperatures. With increasing Prandtl number (P_r), there is a significant reduction in temperature, as shown in Figure 3(b). We consider $P_r > 1$, implying that momentum diffusivity greatly exceeds the thermal diffusivity in the fluid. For greater P_r values, thermal conductivity in the fluid must also decrease, and this explains the decrease in temperature as P_r ascends from 3.97 to 6.2. Thermal boundary layer thickness will therefore also be reduced in the nanofluid sheet regime. With increasing thermal relaxation parameter (γ), the nanofluid temperature is noticeably elevated. Therefore, the Fourier model (γ) evidently under-predicts nanofluid temperatures, whereas the non-Fourier model ($\gamma > 0$) produces greater magnitudes of temperature. The implications for materials processing is that a better estimate of actual temperatures can be achieved with the non-Fourier (*Cattaneo–Christov*) model via a relative simple modification of the heat conduction model. This may have an impact on better designing nanomaterials for specific applications.

Figure 4(a)-(c) illustrates the combined effects of a number of thermophysical parameters on the nanoparticle volume fraction (species concentration), $\phi(\eta)$, in the boundary layer. An increase in Schmidt number (Sc) as displayed in Figure 4(a) clearly enhances the nanoparticle volume fraction, i.e. encourages nanoparticle diffusion in the boundary layer. Nanoparticle species (concentration) boundary layer thickness will therefore also be increased. Schmidt number embodies the ratio of momentum diffusivity to species (nanoparticle) diffusivity. When $Sc > 1$, as studied in this paper, momentum diffusion rate exceeds the species diffusion rate. As Sc increases from 6 to 7, this results in slower nanoparticle migration which manifests in depleted concentrations of nanoparticles, although a more homogenous distribution throughout the boundary layer transverse to the sheet plane is achieved. Schmidt number is therefore a key parameter via which nanoparticle transport can be manipulated. Increasing thermal buoyancy ratio (G_r)

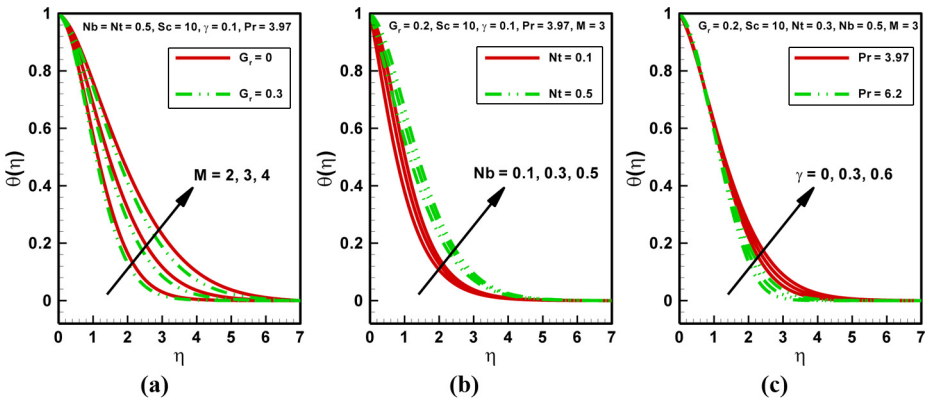

Figure 3.
Temperature profiles for different values of (a) Hartmann number (M) and thermal buoyancy ratio (G_r); (b) Brownian motion parameter (N_b) and thermophoresis parameter (N_t) and (c) thermal relaxation time (γ) and Prandtl number (P_r)

generates a similar effect and also reduces nanoparticle volume fraction. Therefore, greater thermal buoyancy force simultaneously decreases nanoparticle concentration boundary layer thickness. In Figure 4(b), we observe that while increasing thermophoresis parameter (N_t) substantially boosts the nanoparticle concentration, an increase in Brownian motion parameter (N_b) has the contrary influence and considerably suppresses nanoparticle volume fraction magnitudes. With an increase in Prandtl number (P_r) as shown in Figure 4(c), the nanoparticle volume fraction is initially elevated in proximity to the wall, but thereafter, the effect is reversed as we approach the free stream. Further from the wall, the nanoparticle (volume fraction) magnitudes are slightly decreased. With greater thermal relaxation effect, in Figure 4(c), there is a weak elevation in nanoparticle concentration values. This is understandable, as the effect is achieved indirectly via the coupling of the energy and species diffusion boundary layer equations. The prominent influence of thermal relaxation is on temperatures and a diminished effect is sustained therefore by the nanoparticle concentration field.

Figure 5 presents the evolution in skin friction (dimensionless surface shear stress), i.e. velocity gradient at the wall, with Hartmann number (M) and thermal buoyancy ratio (G_r). There is a strong elevation in skin friction with greater magnetic field strength to which Hartmann number is proportional. The profiles are all linear and maximized at low values of thermal buoyancy ratio and minimized at high values of thermal buoyancy ratio. Clearly therefore, increasing thermal buoyancy effect decelerates the boundary layer flow (decreases skin friction) and also serves to elevate momentum boundary layer thickness.

Figure 6(a)-(c) shows the response in wall heat transfer rate, i.e. Nusselt number with various thermophysical parameters. In Figure 6(a), an increase in Hartmann number (M) clearly suppresses Nusselt number, implying a decrease in heat transported to the wall. This agrees with our earlier computations of temperature response [Figure 3(a)], as a higher magnetic field body force will heat the nanofluid boundary layer and this will transfer heat into the body of the fluid away from the wall. Higher thermal relaxation (γ) values again also induce a fall in Nusselt number values, and this is explained by the increase in temperatures [Figure 3(c)] described earlier. This causes a decrease in Nusselt number at the wall. Higher thermal buoyancy ratio (G_r), however, elevates Nusselt number, and physically, this is consistent with the depletion in temperatures computed in Figure 3(a) with greater thermal buoyancy force effect. With increasing thermophoresis parameter (N_t), as plotted in

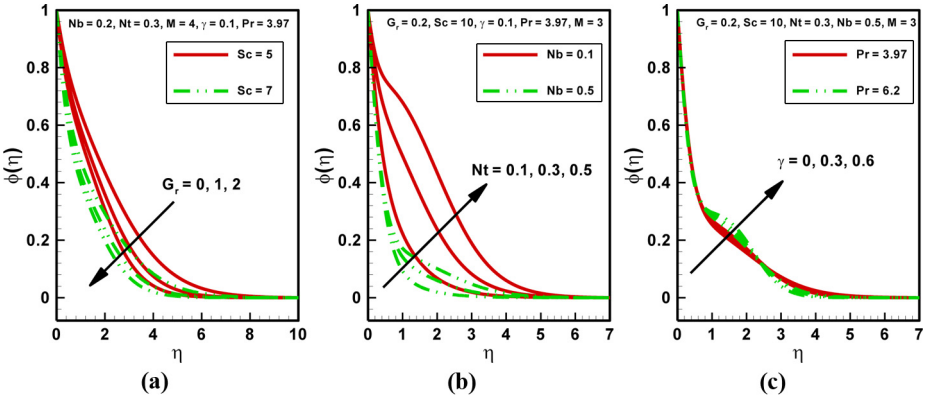

Figure 4.
Nanoparticle volume fraction (species concentration) profiles for different values of (a) Thermal buoyancy ratio (G_r) and Schmidt number (Sc); (b) Brownian motion parameter (N_b) and thermophoresis parameter (N_t) and (c) thermal relaxation time (γ) and Prandtl number (P_r)

Figure 6(b), Nusselt number is also depressed and again this is due to the elevation in temperatures within the nanofluid boundary layer regime with greater thermophoretic effect (as computed earlier in Figure 3(b). With stronger Brownian motion (higher N_b values), again Nusselt number is reduced and once again this is directly attributable to the elevation in temperatures within the nanofluid sheet [Figure 3(b)]. Heat transfer rate to the wall must therefore simultaneously decrease. Figure 6(c) shows that Nusselt number is enhanced with greater Prandtl number (P_r) but suppressed with greater Schmidt number. Increasing thermal buoyancy force (higher G_r values), however, generates a steady ascent in Nusselt number magnitudes, implying that greater heat is transferred to the sheet (wall) with larger thermal buoyancy force, as the boundary layer is cooled and thermal boundary layer thickness is decreased.

Figure 7(a)-(c) presents the evolution of local Sherwood number (dimensionless nanoparticle wall mass transfer rate) with various thermal, magnetic and nanoscale parameters. Increasing Hartmann magnetic parameter (M) is found to considerably reduce

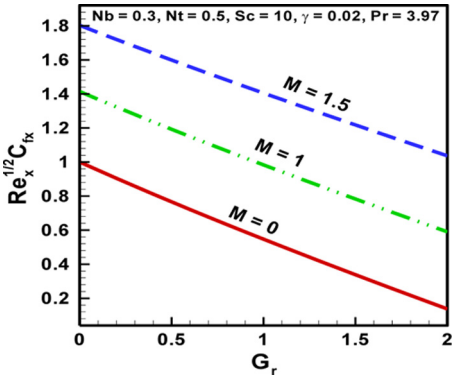

Figure 5.
Skin friction coefficient for different values of Hartmann number (M) and thermal buoyancy ratio (G_r)

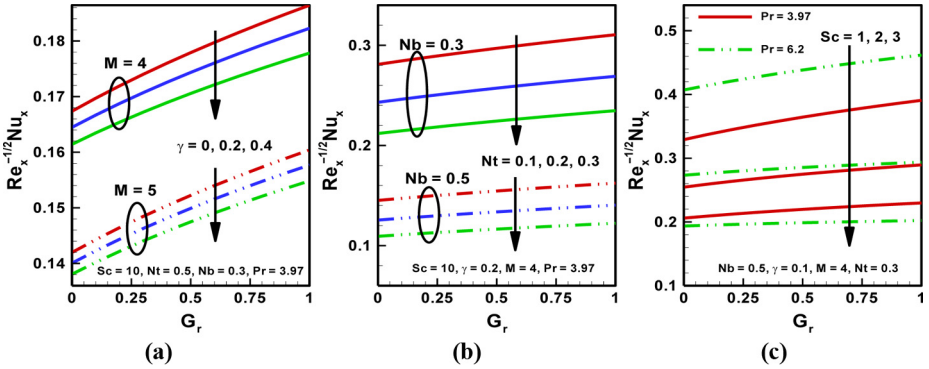

Figure 6.
Nusselt number for different values of (a) non-dimensional thermal relaxation time (γ), Hartmann number (M) and thermal buoyancy ratio (G_r); (b) Brownian motion parameter (N_b), thermophoresis parameter (N_t) and thermal buoyancy ratio (G_r) and (c) Schmidt number (Sc), Prandtl number (P_r) and thermal buoyancy ratio (G_r)

Sherwood number, i.e. greater magnetic field applied transverse to the sheet results in a decreased migration of nanoparticles towards the wall, as nanoparticle concentrations in the boundary layer are elevated (as shown earlier). Conversely, greater thermal relaxation time (γ) very strongly enhances local Sherwood number magnitudes, for any magnetic field scenario. Evidently, greater thermal relaxation, therefore, encourages mass diffusion of nanoparticles towards the wall (sheet). With greater thermal buoyancy effect (higher G_r values), local Sherwood number is also markedly and steadily elevated as testified to by the linear nature of the ascending profiles. Figure 7(b) shows that with increasing Brownian motion parameter (N_b), there is a strong elevation in local Sherwood number values, irrespective of the values of thermophoresis parameter (N_t) and thermal buoyancy ratio (G_r). This increase is due to the elevated migration of nanoparticles towards the wall with greater Brownian motion (smaller particle size) effect. On the other hand, an increase in thermophoresis parameter (N_t) generates the opposite effect and significantly depresses local Sherwood number, as it elevates nanoparticle concentrations within the nanofluid body regime. An increase in G_r values (greater thermal buoyancy effect) consistently enhances mass transfer rates to the wall and results in an increase in local Sherwood number magnitudes. Figure 7(c) shows that while increasing Schmidt number elevates the local Sherwood number values very considerably, a rise in Prandtl number has the converse effect (although weaker) and noticeably reduces local Sherwood number. Increasing thermal buoyancy ratio (G_r) once again achieves a steady elevation in local Sherwood number magnitudes, although the rate of ascent is much less pronounced than that shown in Figures 7(a) and (b).

5. Conclusions

A mathematical model has been developed to simulate the steady, laminar, MHD, incompressible electrically conducting nanofluid flow, heat and mass transfer from a stretching sheet in the presence of a transverse static magnetic field. The *Buongiorno* nanofluid formulation has been adopted which invokes a species diffusion equation for the nanoparticle migration. The non-Fourier Cattaneo–Christov heat flux model has also been

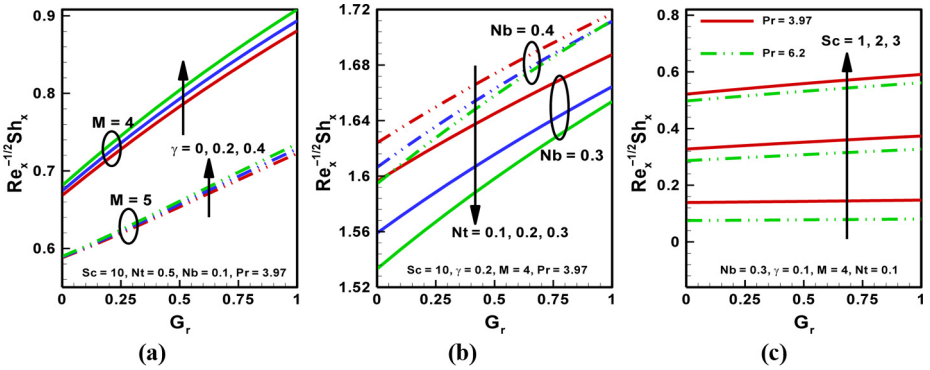

Figure 7.
Local Sherwood number for different values of (a) non-dimensional thermal relaxation time (γ), Hartmann number (M) and thermal buoyancy ratio (G_r); (b) Brownian motion parameter (N_b), thermophoresis parameter (N_t) and thermal buoyancy ratio (G_r) and (c) Schmidt number (Sc), Prandtl number (P_r) and thermal buoyancy ratio (G_r)

used to provide a more realistic estimation of temperature distribution in actual nanofluids. Via suitable scaling transformations and the deployment of carefully selected dimensionless variables, the dimensionless nonlinear partial differential conservation equations have been transformed to an ordinary differential boundary value problem with appropriate boundary conditions. A numerical solution has been presented based on an optimized fourth-order Runge–Kutta algorithm combined with shooting quadrature. The solutions have been validated, where possible, with earlier published results for non-magnetic and forced convection (buoyancy absent) scenarios. The emerging boundary value problem has been shown to be dictated by a number of key thermophysical parameters, namely, Hartmann (magnetic body force) number, thermal buoyancy ratio, thermal relaxation time parameter, Schmidt number, thermophoresis parameter, Prandtl number and Brownian motion number. The influence of these parameters has been computed for velocity, skin friction, temperature, Nusselt number, Sherwood number and nanoparticle concentration distributions. The present investigation has shown that:

- Increasing Brownian motion parameter strongly elevates temperatures and local Sherwood number values, whereas it decreases nanoparticle volume fraction and Nusselt number values.
- Increasing magnetic parameter is found to decelerate the boundary layer flow (i.e. reduce velocities) and also reduce heat transfer rate at the wall (Nusselt number), whereas it enhances temperatures and local Sherwood number magnitudes.
- Increasing thermal buoyancy parameter significantly decreases nanoparticle volume fraction, whereas it weakly reduces temperatures in the nanofluid.
- Increasing thermal relaxation time (i.e. the non-Fourier model) markedly elevates temperatures throughout the boundary layer, whereas initially it weakly increases nanoparticle volume fraction (species concentration) and thereafter slightly depresses magnitudes towards the boundary layer-free stream. The Fourier heat conduction model (vanishing thermal relaxation time) under-predicts temperatures compared with the non-Fourier model.
- Increasing thermophoresis parameter increases both temperatures and nanoparticle volume fraction, whereas it decreases both Nusselt number and local Sherwood number.
- Increasing Schmidt number reduces Nusselt number, whereas it elevates the local Sherwood number.
- Increasing Prandtl number strongly elevates Nusselt number, whereas it weakly reduces the local Sherwood number; and
- The present study has been confined to Newtonian nanofluids. Future investigations will consider rheological aspects and will be communicated imminently.

References

Akbar, N.S., Abdelhalim, E. and Khan, Z.H. (2015), "Numerical analysis of magnetic field effects on eyring-powell fluid flow towards a stretching sheet", *Journal Magnetism and Magnetic Materials*, Vol. 382, pp. 355-358.

Akbar, N.S., Khan, Z.H., Nadeem, S. and Khan, W.A. (2016), "Double-diffusive natural convective boundary-layer flow of a nanofluid over a stretching sheet with magnetic field", *International Journal of Numerical Methods for Heat and Fluid Flow*, Vol. 26 No. 1, pp. 108-121.

Akbar, N.S., Nadeem, S., Hayat, T. and Hendi, A.A. (2012), "Simulation of heating scheme and chemical reactions on the peristaltic flow of an eyring-powell fluid", *International Journal of Numerical Methods for Heat and Fluid Flow*, Vol. 22 No. 6, pp. 764-776.

Bég, O.A., Gorla, R.S.R., Prasad, V.R., Vasu, B. and Prashad, R.D. (2011), "Computational study of mixed thermal convection nanofluid flow in a porous medium", 12th UK National Heat Transfer Conference, *Chemical Engineering Department, University of Leeds*, 30th August-1st September.

Bég, O.A., Ferdows, M., Shamima Islam, S. and Nazrul Islam, M. (2014a), "Numerical simulation of marangoni magnetohydrodynamic bio-nanofluid convection from a non-isothermal surface with magnetic induction effects: a bio-nanomaterial manufacturing transport model", *Journal of Mechanics Medicine Biology*, Vol. 14 No. 3.

Bég, O.A., Motsa, S.S., Islam, M.N. and Lockwood, M. (2014b), "Pseudo-spectral and variational iteration simulation of exothermically-reacting rivlin-ericksen viscoelastic flow and heat transfer in a rocket propulsion duct", *Computational Thermal Sciences*, Vol. 6 No. 1, pp. 1-12.

Bég, O.A., Zueco, J., Norouzi, M., Davoodi, M., Joneidi, A.A. and Assma, F. (2014c), "Elsayed, network and Nakamura tridiagonal computational simulation of electrically-conducting biopolymer micro-morphic transport phenomena", *Computers in Biology and Medicine*, Vol. 44, pp. 44-56.

Bhargava, R., Sharma, S., Anwar Bég, O. and Zueco, J. (2010), "Finite element study of nonlinear two-dimensional deoxygenated biomagnetic micropolar flow", *Communications in Nonlinear Science and Numerical Simulation Journal*, Vol. 15 No. 3, pp. 1210-1233.

Buongiorno, J. and Hu, L.W. (2007), *Nanofluids for Enhanced Economics and Safety of Nuclear Reactors*, Massachusetts Institute of Technology, USA Technical Report.

Buongiorno, J. (2006), "Convective transport in nanofluids", *ASME Journal Heat Transfer*, Vol. 128 No. 3, pp. 240-250.

Cattaneo, C. (1948), "Sulla conduzionedelcalore", *In: Atti del Seminario Matematico e Fisico dell Universita di Modena e Reggio Emilia*, Vol. 3, pp. 83-101.

Choi, S. (1995), "Enhancing thermal conductivity of fluids with nanoparticle. in: developments and applications of non-Newtonian flow", *ASME Fluids Engineering Division*, Vol. 231, pp. 99-105.

Christov, C.I. (2009), "On frame indifferent formulation of the Maxwell–Cattaneo model of finite-speed heat conduction", *Mechanics Research Communications*, Vol. 36 No. 4, pp. 481-486.

Ciarletta, M. and Straughan, B. (2010), "Uniqueness and structural stability for the Cattaneo–Christov equations", *Mechanics Research Communications*, Vol. 37 No. 5, pp. 445-447.

Ellahi, R., Gulzar, M. and Sheikholeslami, M. (2014), "Effects of heat transfer on peristaltic motion of Oldroyd fluid in the presence of inclined magnetic field", *Journal of Magnetism and Magnetic Materials*, Vol. 372, pp. 97-106.

Elsayed, A.F. and Anwar Bég, O. (2014), "New computational approaches for biophysical heat transfer in tissue under ultrasonic waves: variational iteration and Chebyshev spectral simulations", *J. Mechanics Medicine Biology*, Vol. 14 No. 3, pp. 17.

Ferdows, M., Khan, M.S. and Anwar Bég, O. (2014), "Numerical study of transient magnetohydrodynamic radiative free convection nanofluid flow from a stretching permeable surface", *Proceedings of the Institution of Mechanical Engineers, Part E: Journal of Process Mechanical Engineering*, Vol. 228 No. 3, pp. 181-196.

Frizen, V.E. and Sarapulov, F.N. (2010), "Formation of MHD processes in induction crucible furnace at single-phase supply of inductor", *Russian Electrical Engineering*, Vol. 81 No. 3, pp. 159-164.

Gorla, R.S.R. and Sidawi, I. (1994), "Free convection on a vertical stretching surface with suction and blowing", *Journal of Applied Sciences Research*, Vol. 52 No. 3, pp. 247-257.

Han, S., Zheng, L., Li, C. and Zhang, X. (2014), "Coupled flow and heat transfer in viscoelastic fluid with Cattaneo–Christov heat flux model", *Applied Mathematics Letters*, Vol. 38, pp. 87-93.

Hoque, M.M., Md Mahmud, A., Ferdows, M. and Anwar Bég, O. (2013), "Numerical simulation of dean number and curvature effects on magneto-biofluid flow through a curved conduit", *Proc. IMECHE – Part H; J. Engineering in Medicine*, Vol. 227 No. 11, pp. 1155-1170.

Huminic, G. and Huminic, A. (2012), "Application of nanofluids in heat exchangers: a review", *Renewable and Sustainable Energy Reviews*, Vol. 16 No. 8, pp. 5625-5638.

Kandasamy, R., Loganathan, P. and Puvi Arasu, P. (2011), "Scaling group transformation for MHD boundary-layer flow of a nanofluid past a vertical stretching surface in the presence of suction/injection", *Nuclear Engineering and Design*, Vol. 241 No. 6, pp. 2053-2059.

Khan, W.A. and Pop, I. (2010), "Boundary-layer flow of a nanofluid past a stretching sheet", *International Journal of Heat and Mass Transfer*, Vol. 53 Nos 11/12, pp. 2477-2483.

Khan, Z.H., Khan, W.A. and Culham, R.J. (2014), "Estimation of boundary-layer flow of a nanofluid past a stretching sheet: a revised model", *Journal of. Hydrodynamics*, (in press).

Kim, S.J., Bang, I.C., Buongiorno, J. and Hu, L.W. (2007), "Study of pool boiling and critical heat flux enhancement in nanofluids", *Bulletin of The Polish Academy of Sciences Technical Sciences*, Vol. 55 No. 2, pp. 20-30.

Latiff, N.A., Uddin, M.J., Anwar Bég, O. and Ahmad Izani, M.I. (2016), "Unsteady forced bioconvection slip flow of a micropolar nanofluid from a stretching/shrinking sheet", *Proc. IMechE – Part N: J. Nanoengineering and Nanosystems*, Vol. 230 No. 4, pp. 1-10, doi: 10.1177/1740349915613817.

Mustafa, M. (2015), "Cattaneo–Christov heat flux model for rotating flow and heat transfer of upper-convected Maxwell fluid", *AIP Advances*, Vol. 5 No. 4, p. 047109

Nadeem, S., Mehmood, R. and Akbar, N.S. (2013), "Non-orthogonal stagnation point flow of a nano non-Newtonian fluid towards a stretching surface with heat transfer", *International Journal Heat Mass Transfer*, Vol. 57 No. 2, pp. 679-689.

Nadeem, S., Mehmood, R. and Akbar, N.S. (2015), "Oblique stagnation flow of Jeffery fluid over a stretching convective surface: optimal solution", *International Journal of Numerical Methods for Heat and Fluid Flow*, Vol. 25 No. 3, pp. 454-471.

Narvaez, J.A., Veydt, A.R. and Wilkens, R.J. (2014), "Evaluation of nanofluids as potential novel coolant for aircraft applications: the case of de-ionized water-based alumina nanofluids", *ASME J. Heat Transfer*, Vol. 136 No. 5, p. 051702.

Nield, D.A. and Kuznetsov, A.V. (2009), "The Cheng–Minkowycz problem for natural convective boundary-layer flow in a porous medium saturated by a nanofluid", *International Journal Heat Mass Transfer*, Vol. 52 Nos 25/26, pp. 5792-5795.

Prasad, V.R., Gaffar, S.A. and Anwar Bég, O. (2015), "Non-similar computational solutions for free convection boundary-layer flow of a nanofluid from an isothermal sphere in a non-Darcy porous medium", *Journal of Nanofluids*, Vol. 4 No. 2, pp. 1-11.

Rana, P. and Bhargava, R. (2012), "Flow and heat transfer over a nonlinearly stretching sheet: a numerical study", *Communications in Nonlinear Science and Numerical Simulation*, Vol. 17 No. 1, pp. 212-226.

Rana, P., Bhargava, R. and Anwar Bég, O. (2013), "Finite element simulation of unsteady magneto-hydrodynamic transport phenomena on a stretching sheet in a rotating nanofluid", *Proceedings of the Institution of Mechanical Engineers Part N Journal of Nanoengineering and Nanosystems*, Vol. 227, pp. 77-99.

Rashidi, M.M., Freidoonimehr, N., Hosseini, A., Anwar Bég, O. and Hung, T.K. (2014), "Homotopy simulation of nanofluid dynamics from a non-linearly stretching isothermal permeable sheet with transpiration", *Meccanica*, Vol. 49 No. 2, pp. 469-482.

Sakiadis, B.C. (1961), "Boundary layer behavior on continuous solid surfaces. II: the boundary layer on a continuous flat surface", *AIChE Journal*, Vol. 7 No. 2, pp. 221-225.

Salahuddin, T., Malik, M.Y., Hussain, A., Bilal, S. and Awais, M. (2016), "MHD flow of Cattaneo–Christov heat flux model for Williamson fluid over a stretching sheet with variable

thickness: using numerical approach", *Journal Magnetism and Magnetic Materials*, Vol. 401, pp. 991-997.

Sheikholeslami, M., Bandpy, M.G., Ellahi, R. and Zeeshan, A. (2014a), "Simulation of MHD CuO-water nanofluid flow and convective heat transfer considering Lorentz forces", *Journal of Magnetism and Magnetic Materials*, Vol. 369, pp. 69-80.

Sheikholeslami, M., Ellahi, R., Hassan, M. and Soleimani, S. (2014b), "A study of natural convection heat transfer in a nanofluid filled enclosure with elliptic inner cylinder", *International Journal of Numerical Methods for Heat & Fluid Flow*, Vol. 24 No. 8, pp. 1906-1927.

Sheikholeslami, M., Ganji, D.D., Bandpy, G.T., Farooq, M.A., Alsaedi, A. and Al-Solamy, F. (2014c), "Magnetic field effects on nanofluid flow, and heat transfer using KKL model", *Journal of Taiwan Institute of Chemical Engineers*, Vol. 45 No. 3, pp. 795-807.

Sheikholeslami, M., Ganji, D.D., Gorji-Bandpy, S. and Soleimani, M. (2014d), "Magnetic field effect on nanofluid flow and heat transfer using KKL model", *Journal of the Taiwan Institute of Chemical Engineers*, Vol. 45 No. 3, pp. 795-807.

Sheikholeslami, M., Gorji, M., Bandpy Ellahi, R., Hassan, M. and Soleimani, S. (2014e), "Effects of MHD on cu-water nanofluid flow and heat transfer by means of CVFEM", *Journal of Magnetism and Magnetic Materials*, Vol. 349, pp. 188-200.

Straughan, B. (2010), "Thermal convection with the Cattaneo–Christov model", *International Journal Heat Mass Transfer*, Vol. 53 Nos 1/3, pp. 95-98.

Takhar, H.S., Agarwal, R.S., Bhargava, R. and Jain, S. (1998), "Mixed convection flow of a micropolar fluid over a stretching sheet", *Heat and Mass Transfer*, Vol. 34 Nos 2/3, pp. 213-219.

Togun, H., Ahmadi, G., Abdulrazzaq, T., Shkarah, A.J., Kazi, S.N., Badarudin, A. and Safaei, M.R. (2015), "Thermal performance of nanofluid in ducts with double forward-facing steps", *Journal of the Taiwan Institute of Chemical Engineers*, Vol. 47, pp. 28-42.

Uddin, M.J., Anwar Bég, O. and Ismail, A.I. (2015), "Radiative-convective nanofluid flow past a stretching/shrinking sheet with slip effects", *AIAA Journal Thermophysics Heat Transfer*, Vol. 29 No. 3, pp. 513-523.

Wang, C.Y. (1989), "Free convection on a vertical stretching surface", *ZAMM-Journal of Applied Mathematics and Mechanics*, Vol. 69 No. 11, pp. 418-420.

Zeeshan, A., Majeed, A. and Ellahi, R. (2016), "Effect of magnetic dipole on viscous ferro-fluid past a stretching surface with thermal radiation", *Journal of Molecular Liquids*, Vol. 215, pp. 549-554.

Corresponding author
Noreen Sher Akbar can be contacted at: noreensher@yahoo.com